Analytica Chimica Acta 713 (2012) 115–120

Contents lists available at SciVerse ScienceDirect

Analytica Chimica Acta

journal homepage: www.elsevier.com/locate/aca

Simultaneous impedimetric and amperometric interrogation of renal cells exposed to a calculus-forming salt

Szilveszter Gáspár*, Sorin David, Cristina Polonschii, Irene Marcu, Mihaela Gheorghiu, Eugen Gheorghiu

International Centre of Biodynamics, 1B Intrarea Portocalelor Street, 060101 Bucharest, Romania

ARTICLE INFO

Article history:
Received 16 December 2010
Received in revised form 9 November 2011
Accepted 10 November 2011
Available online 25 November 2011

Keywords:
Superoxide biosensor
Impedance spectroscopy
Amperometric detection
Renal cells
Oxidative stress
Cellular adherence

ABSTRACT

The complexity of the cellular response, induced even by the simplest experimental stimulus, requires an increased number of cellular parameters to be simultaneously monitored. An all electrochemical system allowing the simultaneous and real-time monitoring of both cell adherence and superoxide release into the extracellular space was developed to address this challenge. Cell adherence (to neighboring cells and to substrate) was monitored using non-faradaic impedance spectroscopy while the superoxide release was monitored using a cytochrome c-based amperometric biosensor. The system was used to observe for the first time how these two cellular parameters are changing in real-time for renal cells exposed to calcium oxalate, a calculus-forming salt. It was discovered that calcium oxalate crystals decrease cell adherence and in the same time induce oxidative stress by an overproduction of superoxide. Subconfluent cells, without fully developed tight junctions, appear to be more vulnerable than confluent cells with tight junctions indicating the important protective role of these junctions.

1. Introduction

Scientific instrumentation is commonly tuned for the determination of one parameter or of a relatively low number of akin parameters which are most often determined based on the same detection principle (e.g. there are analyzers which simultaneously measure oxygen consumption, extracellular acidification, and carbon dioxide production with fluorescence-based optical sensors [1]). Microarray-based tools are delivering plenty of data but again based on the same detection principle, about the same type of interaction (e.g. DNA-target), and with no hint on the process dynamics. In cell biology, where even the simplest stimulus induces a myriad of changes in a living cell, this can be frustrating because, in their quest to the complete picture on cellular behavior, researchers are forced to sequentially investigate interconnected processes which occur in parallel. Moreover, very often cell biologists access only endpoints because their tools cannot deliver appropriate temporal resolution. Therefore we report on a novel analytical platform which combines two different detection principles and monitors two very different cellular parameters, namely cell adherence and superoxide release into the extracellular space. The evolution of the cellular adherence is evaluated in real-time using non-faradaic impedance spectroscopy while the superoxide release is evaluated in real-time using cytochrome c-based amperometric biosensors.

Impedance spectroscopy was previously used (among many other applications) to monitor cell membrane capacitance [2], to determine the cell-to-substrate [3] or cell-to-cell gaps [4], to study the inhibitory effects of a human neuropeptide [5], to develop a wound-healing assay [6], to observe the interaction of red blood cells with bovine pulmonary artery endothelial cells [7], and to test the cytotoxicity of some chemicals [8].

Amperometric sensors made their way into cell biology through carbon fiber microelectrodes used to reveal details of neurotransmission [9] and then Pt microelectrodes used to measure reactive oxygen species [10]. The already mentioned superoxide is most often detected with amperometric sensors consisting of a gold electrode bearing covalently immobilized cytochrome c. Such sensors were already proved to have minimal interferences from hydrogen peroxide, ascorbic acid, and uric acid [11–14], to perform well even *in vivo* [15], and to be sensitive enough to measure the small amounts of superoxide produced by cells [16–18]. Therefore, a similar sensor is used in the present work. However, the selectivity of the cytochrome c-based superoxide sensor against other potential interferents such as nitric oxide and peroxynitrite was not determined. The generation of nitric oxide and of peroxynitrite by renal cells exposed to calcium oxalate cannot be ruled out and thus deserves further investigation.

Impedance spectroscopy and amperometry have thus matured into reliable methods for investigating cellular processes. However, they were very seldom combined for simultaneous measurements [19–21], and none of the previously reported dual (i.e. both impedimetric and amperometric) monitoring systems reveals signs of

* Corresponding author. Tel.: +40 021 3104364; fax: +40 021 3104361.
E-mail address: sgaspar@biodyn.ro (S. Gáspár).

0003-2670/$ – see front matter © 2011 Elsevier B.V. All rights reserved.
doi:10.1016/j.aca.2011.11.031

oxidative stress (or uses sensors bearing biorecognition elements). Taking into account the complex role of reactive oxygen species in biology [22], it was one of the aims of the present work to extend multiparametric monitoring concepts to superoxide. The involvement of the oxidative stress also in the cellular damage caused by calcium oxalate is sustained by a growing body of evidence [23]. However, many other details of renal calculi formation and of the mechanism of cellular damage by renal calculi are not known. Therefore, the calcium oxalate–renal cell interaction is the subject of many scientific endeavors (e.g. [23–25]), including the one described in the present work.

2. Materials and methods

2.1. Materials

3,3′-Dithiodipropionic acid, cytochrome c, aminopropyl glass (average pore size 170 Å, 200–00 mesh), HEPES, potassium chloride, calcium chloride, and sodium chloride were purchased from Sigma Aldrich Inc. (USA). N-(3-dimethylaminopropyl)-N′-ethylcarbodiimide hydrochloride (EDC), and N-hydroxysuccinimide (NHS) were purchased from Fluka Chemie GmbH (Switzerland). Calcium oxalate was purchased from Aldrich Chemical Company Inc. (USA). All aqueous solutions were prepared using ultrapure water from a Direct-Q® 3 UV system from Millipore S.A.S. (France). The working buffer of pH 7.4 consisted of 100 mM NaCl, 5 mM HEPES, 1 mM $CaCl_2$, and 2 mM KCl.

Experiments were carried out on A6 cells (epithelial cells from the *Xenopus levis* kidney) grown at 28 °C, and 1% CO_2 in a humidified incubator. Cells were grown onto glass cover slips (22 mm × 22 mm × 0.17 mm, Carl Roth GmbH, Germany) bearing electrodes for performing impedance spectroscopy. No treatment of the gold surfaces was necessary to assure cell adherence. Growth medium was renewed twice weekly and consisted of a 1:1 mixture of Leibovitz's L-15 (Gibco brand, from Invitrogen, USA) and Ham's F-12 media (Gibco, Invitrogen), supplemented with 10% fetal bovine serum (Gibco, Invitrogen), 2.6 mM $NaHCO_3$ (Gibco, Invitrogen), 3.8 mM glutamine (Gibco, Invitrogen), 95 U mL^{-1} penicillin and 95 μg mL^{-1} streptomycin (Pen Strep, Gibco, Invitrogen).

2.2. Measuring chamber and method

Being aware of a significant electrical crosstalk between impedance spectroscopy and amperometry experiments performed in the same solution, a measuring chamber with two identical compartments was fabricated (Fig. 1).

Its base consisted of a glass cover slip (22 mm × 22 mm × 0.17 mm). Thin film technology was used to pattern four sets of Au working and counter electrodes for on-chip impedance spectroscopy onto such cover slips. The circular counter electrodes surround the 3 mm diameter disk working electrodes for a uniform distribution of the electric field. Two-component poly(dimethylsiloxane) (PDMS, Sylgard 184 from Dow Corning Corporation, USA) and an appropriate mould were used to fabricate two wells of 250 μL each. Amperometry was performed with an external set of electrodes. The counter electrode consisted of a 1 mm Pt wire. The reference electrode was a 2 mm diameter Ag/AgCl, 3 M KCl electrode (DRIREF-2SH from WPI Inc., USA). The working electrode consisted of the superoxide biosensor fabricated as previously described by us [17]. Briefly, cylindrical gold electrodes (diameter of 0.8 mm and height of 4 mm) were carefully cleaned and then modified with a self-assembled monolayer (SAM) of 3,3′-dithiodipropionic acid. The carboxyl groups of the SAM were activated using EDC and NHS chemistry. In the last step, cytochrome c was covalently attached to the activated carboxyl moieties of the SAM.

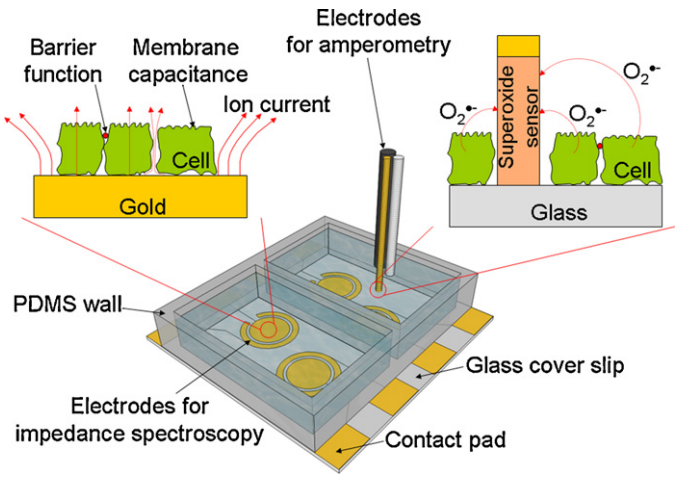

Fig. 1. Two-compartment measuring chamber (with a footprint of only 22 mm × 22 mm) for the dual interrogation of cells. One of the compartments is used to monitor cells using non-faradaic impedance spectroscopy while the other is used to monitor cells using an amperometric superoxide sensor.

2×10^5 cells were seeded into each compartment of the measuring chamber and left to grow into a subconfluent (2–3 days) or confluent layer (4–7 days). Before dual measurements, the culture medium was removed and cells were gently washed with the working buffer. The electrodes for amperometry were lowered into one of the compartments of the measuring chamber using a micromanipulator (model HS6 from WPI Inc., USA). The tip of the superoxide biosensor was always brought into contact with the cells in order to assure a reproducible positioning (however, due to the small lateral dimension of the sensor, only an insignificant number of cells were damaged). The electrodes for impedance spectroscopy and the superoxide sensor were both subsequently polarized (using a 4294 A Precision Impedance Analyzer from Agilent Technologies Ltd., Japan, and a VSP potentiostat equipped with a low-current module from Bio-Logic S.A.S., France, respectively). An alternative current potential with zero bias, a root mean square amplitude of 20 mV, and frequency from 400 Hz to 600 000 Hz was used in impedance spectroscopy. Recording one full impedance spectrum took between 2 and 5 s (depending on the number of frequencies investigated). A potential of 150 mV was applied onto the superoxide biosensor and two current values were recorded every second. Once a stable background signal was obtained, calcium oxalate was added to both compartments of the chamber and the signal changes were recorded. The calcium oxalate suspension was relatively slowly and drop-wise pipetted all over the surface of the measuring chamber assuring thus an even distribution of the crystals over the cells.

3. Results and discussion

A6 cells grow to confluence and subsequently develop tight junctions. Tight junctions prevent the passage of most molecules and ions through the space between cells. Data from literature also indicates that the viability of renal cells is negatively affected by calcium oxalate. The highest percentage of cell death (90%) for renal cells exposed to calcium oxalate was reported for proximal tubule cells from F-344 rats incubated with 1.47 mg mL^{-1} calcium oxalate for 6 h [26]. However, calcium oxalate commonly induces smaller percentage of cell death in vitro. Taking into account the lower amount of calcium oxalate spread over the cells (0.91 mg mL^{-1}), and the relatively short time scale of our experiments (about 1 h),

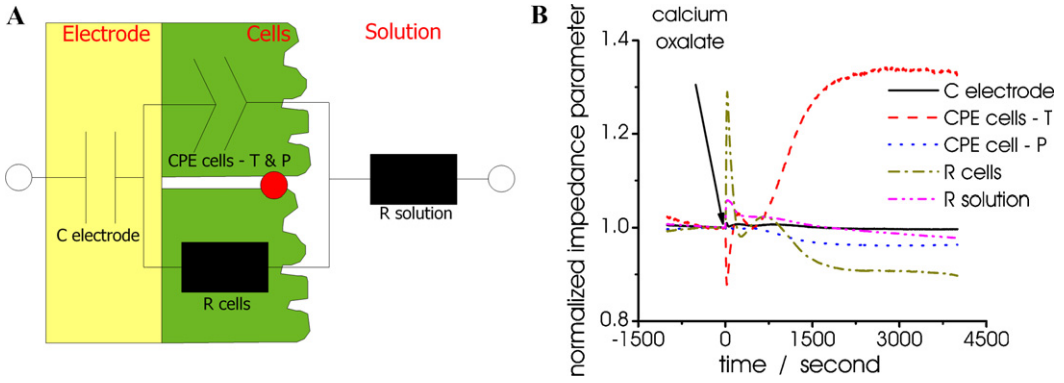

Fig. 2. Equivalent circuit corresponding to a cell-covered electrode (A) and the evolution of its elements when the cells are exposed to calcium oxalate crystals (B). *Conditions*: A6 cells at passage 115 in their 3rd day after seeding were used; the impedance-derived parameters were normalized to the following values recorded just before injecting calcium oxalate: *C electrode* = 2.1×10^{-7} F, *CPE cells-T* = 3.5×10^{-7} s^n Ohm^{-1}, *CPE cells-P* = 0.72, *R cells* = 1112 Ω, *R solution* = 135 Ω; 0.91 mg mL^{-1} calcium oxalate crystals were dispersed over the cells at $t = 0$ s.

cell death cannot be excluded but very probably is not dominating our observations. Attention will be focused on the very initial moments of the cell–crystal encounter, a critical time period that is not usually addressed in studies.

The amperometric biosensor bears cytochrome c in a surface concentration of 11.7 ± 2.9 pmol cm^{-2}, has a linear range of up to 1 μM superoxide, and displays a sensitivity of $18.3 \pm 2.7 \times 10^2$ A m^{-2} M^{-1} as previously determined [17]. The superoxide concentration observed in the extracellular space during our experiments has never exceeded this linear range. The sensor sensitivity can be used to get an approximation of the superoxide concentration. However in our discussions we indicate a variation of the superoxide concentration although the recorded current signal was not converted into superoxide concentration units.

3.1. *Effect of calcium oxalate as evaluated using different equivalent circuits*

An equivalent circuit can be used to advantageously separate the impedance of the cell layer from the other components of the experimentally measured impedance. The equivalent circuit depicted in Fig. 2A not only has a low number of elements as compared to the number of data points in the spectrum (most often 30) but also the elements have physical meaning. Thus, the electrode is described by a capacitance (*C electrode*). The cell layer is described by a constant phase element (*CPE cells*) connected in parallel with a resistance (*R cells*). The constant phase element describing the cells is in turn described by an absolute value *CPE cells-T* and an exponent *CPE cells-P* (see Supplementary data). In our case *CPE cells* replaces the cell membrane capacitance (of both the apical and the basolateral membranes). *R cells* is the transepithelial resistance (which accounts first of all for the paracellular current path). The solution bathing the cells is described by a resistance (*R solution*) that is in series with the elements for the electrode and cells.

If cells are incubated with a compound that negatively affects them, and the physical meaning of each element from the above equivalent circuit is correctly selected, one should expect an increase of *CPE cells-T* (because cells are loosening both their tight junctions and their adherence points to the substrate and thus rounding up and displaying larger surface area), a decrease of *CPE cells-P* (because the non-heterogeneity of the surface increases), and a decrease of *R cells* (because, once the adherence to neighboring cells and to the substrate is affected, additional current flows through the system through the just formed paracellular pathways). The parameters describing the electrode and the solution should stay rather constant during the same time.

All 2011 spectra recorded during the experiment depicted in Fig. 2B were fitted with the above-described equivalent circuit (see also Supplementary data). The good chi-squared values obtained in fitting (from 0.00032 to 0.00058) prove that the selected equivalent circuit describes well the cell-covered electrode both before and after adding calcium oxalate. After adding calcium oxalate *CPE cells-T* increases (+33%) while both *CPE cells-P* and *R cells* decrease (with −4% and −10%, respectively). The parameters associated to the electrode and the solution present variations of maximum 2%. The fact that, the cell-associated elements are more pronouncedly changing than the electrode- and buffer-associated elements after adding calcium oxalate crystals prove that also the physical meaning of the elements was correctly selected. The evolution of the elements of the equivalent circuit suggests a cell swelling followed by a rounding up (with the detachment from neighboring cells and from the substrate) after adding calcium oxalate.

Besides the ideal case of a monolayer of fully confluent cells, it is also interesting to investigate extreme cases such as subconfluent cell layers (2 days old cells) and cells partially grown into multilayers (6–7 days old cells). Such cell layers display quite different and thus interesting structural and functional elements. However they also require two additional equivalent circuits and this makes data comparison more difficult. Therefore, in order to compare the results from all different cell layers, the impedance recorded at 1800 Hz was taken into work (this impedance is strongly affected by the presence of the cells, see Fig. S2 of Supplementary data). Impedance at 1800 Hz was then converted into the resistance (*R p*) and the capacitance (*C p*) of an equivalent parallel RC circuit. Fig. 3 displays the evolution of *R p* and *C p* for the experiment of Fig. 2 together with the amperometric signal recorded in the second compartment of the measuring chamber (containing similarly treated cells).

The evolution of *C p* qualitatively resembles the evolution of *CPE cells-T* and thus we can assume that is dominated by changes in cell membrane capacitance. The evolution of *R p* qualitatively resembles the evolution of *R cells* and thus we can assume that is dominated by changes in transepithelial resistance. Equally important, this simpler approach allows indeed comparing all impedance spectroscopy data from all cell-covered electrodes.

When carefully analyzing Fig. 3, one can observe three distinct regions in both the impedimetric and the amperometric signals:

I. Immediately after injecting the crystals, there are about 5 min during which the steady state background signals are destabilized by the injection itself.
II. About 5 min after injecting the crystals, *R p* slightly increases and *C p* slightly decreases while the superoxide proportional

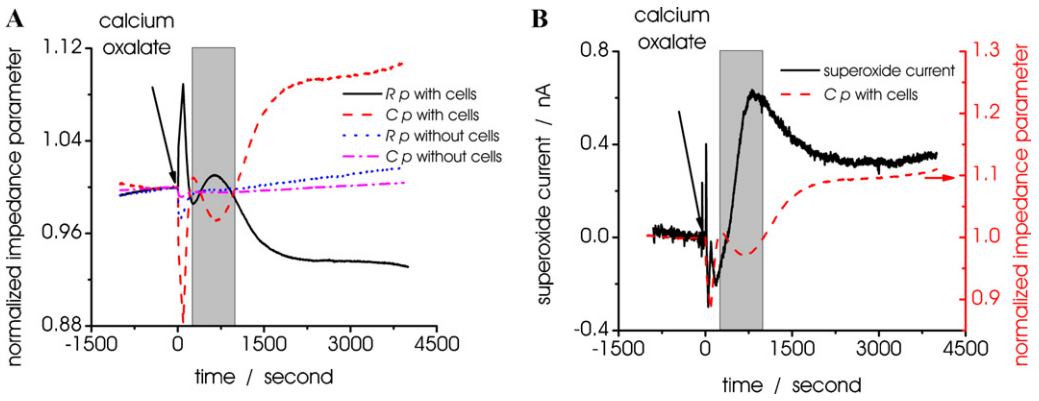

Fig. 3. Evolution of the impedance-derived parameters (A) and of the current signal due to the extracellular superoxide (B) in an experiment involving the incubation of the renal cells with calcium oxalate crystals. *Conditions*: A6 cells at passage 115 in their 3rd day after seeding were used; the impedance-derived parameters were normalized to the following values recorded just before injecting calcium oxalate: $R\,p = 1425\ \Omega$, and $C\,p = 3.5 \times 10^{-7}$ F; 0.91 mg mL^{-1} calcium oxalate crystals were dispersed over the cells at $t = 0$ s.

current begins to rise (see grayed out sections in Fig. 3A and B). A possible cell swelling might explain both the increase of *R p* and decrease of *C p* if this swelling affects more pronouncedly cell height than cell diameter (and thus part of the cell membrane "escapes" the electric field distribution from the close proximity of the electrode). Glass microparticles were found to produce microlesions in the membrane of the cells they land onto [27], and mechanical injury is an event that was found to induce cell swelling [28]. Therefore, it seems plausible that calcium oxalate crystals landing onto cells produce microlesions in the cell membrane as well. This mechanical stress, in turn, produces cell swelling. There is actually one paper reporting cell swelling following exposure to calcium oxalate [29]. Interestingly, what appears to be cell swelling occurs in the same time with the manifestation of an oxidative stress in the extracellular space. This is again not unusual. Cell swelling and oxidative stress have already been found to be interconnected [30]. The extracellular superoxide concentration passes its maximum and starts decaying approximately when the cells seem to return to their original state (15–25 min after injection of the calcium oxalate crystals). It must be also mentioned that the burst of the superoxide into the extracellular space is sometimes not accompanied by a significant volume change in terms of the impedance-derived parameters.

III. In the third signal region, *R p* decreases and *C p* increases indicating that cells are detaching (from the electrodes and from each other) and rounding up. Interestingly, the cell layer seems to enter a steady state (indicated by the lack of evolution in the electrode impedance) about the same time the superoxide vanishes from the extracellular space. On one hand such a behavior suggests a connection between oxidative stress and decreased cell adherence. On the other hand the impedance-derived parameters have the same evolution even when no significant amounts of superoxide are detected in the extracellular space.

Cells have never completely (i.e. visibly) detached from the electrode surface during our experiments.

3.2. Effect of cell age on cellular vulnerability

One interesting question is how cells at different stages of developing tight junctions are reacting to an encounter with calcium oxalate? We have tried to answer this question of biological relevance in order to further prove the usefulness of our dual cell interrogation system. When investigating the evolution of the impedance-derived parameters with cell age for cells not exposed to calcium oxalate crystals two important issues were noticed. First, *R p* increases and *C p* decreases with cell age (not shown). This behavior corresponds to the growth of individual cells (which act as insulating patches with certain surface area on the electrode) into a confluent cell layer (that almost completely insulates the

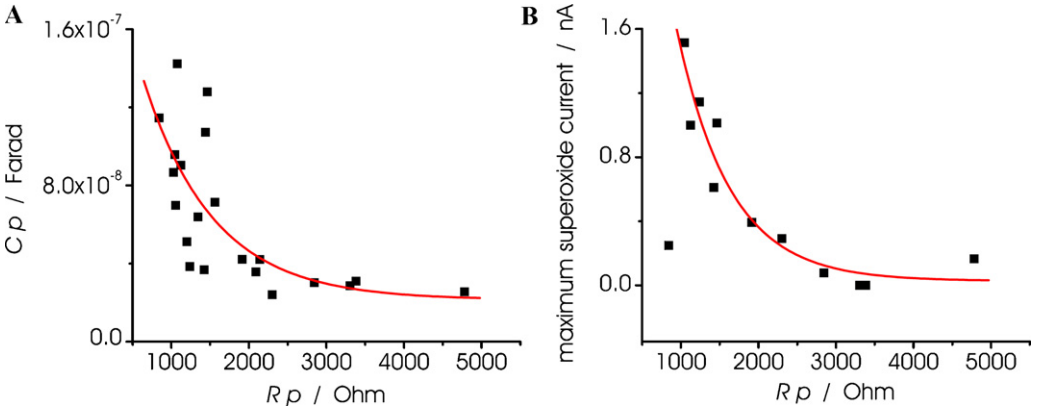

Fig. 4. Evolution of the *C p* impedance-derived parameter (A), and of the maximum superoxide current (B) as a function of *R p* impedance-derived parameter of the renal epithelium. Conditions: A6 cells from different passages (111–123) and of different age were used; impedance data recorded just before adding calcium oxalate is shown; maximum superoxide current signals observed following the dispersion of 0.91 mg mL^{-1} calcium oxalate is shown.

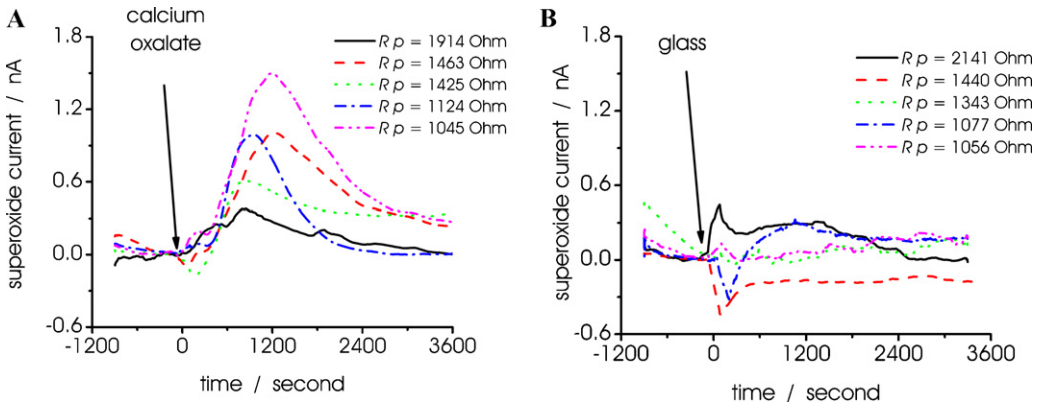

Fig. 5. Current signals corresponding to the superoxide concentration in the extracellular space of renal cells exposed to either calcium oxalate crystals (A) or glass microparticles (B). *Conditions*: A6 cells characterized by about the same impedance-derived parameters were selected to be exposed to either calcium oxalate crystals or glass microparticles (see legends); 0.91 mg mL^{-1} of either calcium oxalate crystals (A) or glass microparticles (B) were dispersed over the cells at $t = 0$ s.

electrode from the buffer and displays a smaller total surface area than the individual cells). Second, there is a significant scattering of the impedance-derived parameters for cells of the same age. This lack of reproducibility in cell growth, which is not unusual with cells from different passages, sustains the usefulness of adding impedance spectroscopy to other methods of monitoring cellular processes. Impedance spectroscopy will give a very precise description of the status of the cell layer. Therefore, Rp of the cell layer was subsequently used instead of its age for comparison purposes.

When representing Cp as a function of Rp for all layers consisting of cells of different age and from different passages (Fig. 4A), it becomes obvious that during the development of the renal epithelium there are two stages from point of view of the impedimetric response.

In the first stage ($Rp < 2000\ \Omega$) we have a significant decrease of Cp that is accompanied by only minor changes of Rp. In the second stage ($Rp > 2000\ \Omega$) we have a significant change of the Rp accompanied by only a slight decrease of Cp. Such a behavior is what one expects from cells which first grow to confluence (accompanied by a significant decrease of the total cell surface area but with a relatively minor effect on transepithelial impedance, because the paracellular current pathways severely dominate the impedance) and then develop tight junctions (accompanied by a tremendous decrease of the cell layer permittivity to ions and molecules, and thus of the current passing the cell layer, but with minor effect on the total surface area of cell membrane).

The different cell layers were subsequently incubated with calcium oxalate. Signals as those shown in Fig. 3 were obtained. Interestingly, when representing the maximum of the superoxide concentration–proportional current as a function of Rp, a pattern that is quite similar to the Cp vs. Rp dependence is emerging (Fig. 4B). This allows concluding that cell layers which are not yet confluent and not yet united by tight junctions are significantly more sensitive to the effect of calcium oxalate (based on the amount of superoxide reaching the extracellular space).

3.3. Is it mechanical stress or chemical stress?

It was also our aim to identify how much of the observed adverse effect is due to the particulate nature of calcium oxalate (mechanical stress) and how much is due to the chemical nature of calcium oxalate (chemical stress). Therefore, similar experiments as those discussed above but with glass microparticles injected instead of calcium oxalate crystals were performed. Interestingly, glass microparticles (with aminopropyl surface chemistry and of 37–74 μm diameter) induced qualitatively the same changes in the impedance of the renal cell layers as calcium oxalate crystals (not shown). However, as shown in Fig. 5, no significant superoxide release was observed in the 5 experiments where glass microparticles were used.

Glass beads, of similar size or larger than used in the present study, were successfully used to temporarily disrupt the cell membrane [27]. The adverse effect noticed in our impedance spectroscopy measurements is most probably due to such mechanical stress. The similar evolution of the impedance-derived parameters in experiments with glass microparticles and with calcium oxalate crystals suggests that calcium oxalate also produces temporary cell membrane disruption. However, next to producing membrane microlesions, calcium oxalate seems to induce also a chain of biochemical events leading to oxidative stress and eventually to the appearance of superoxide in the extracellular space. Glass microparticles seem to not have this ability. Calcium oxalate appears thus to affect renal cells by a combination of mechanical and chemical stress.

4. Conclusions

Although changes in adherence and superoxide overproduction are processes which occur very often when cells are physically of chemically stressed, they were never before simultaneously and in real-time monitored. Therefore, an electrochemical system able to simultaneously monitor these two very different cellular parameters was put together and successfully used to investigate the effect of calcium oxalate crystals on A6 renal cells. It was discovered that calcium oxalate decreases cell adherence and induces oxidative stress that is amperometrically noticeable in the extracellular space. Renal cell layers which are subconfluent and have no fully developed tight junction were found more vulnerable to the effect of calcium oxalate than confluent cell layers. By comparing the effect of calcium oxalate crystals with the effect of glass microparticles, it was found that changes in the cell layer impedance are at least partially due to microlesions of the cell membrane caused by the particles. Therefore, the adverse effect, calcium oxalate crystals have on renal cells, is a mixture of mechanical and chemical stress. Impedance spectroscopy emerged as an excellent method to reveal and then take into account the differences in cell growth rate from one passage to other. The developed system could be useful for investigating the effect of other compounds on various adherently growing cellular models.

Acknowledgement

Financial help from the Romanian National Authority for Scientific Research (through the National Plan for Research Development

and Innovation, contract no. 81-028, 71-073, and 12-121 and through the Sectoral Operational Programme – Increasing Economic Competitiveness, Priority Axis 2, contract no. 157) is acknowledged.

Appendix A. Supplementary data

Supplementary data associated with this article can be found, in the online version, at doi:10.1016/j.aca.2011.11.031.

References

[1] Y. Abe, T. Sakairi, H. Kajiyama, S. Shrivastav, C. Beeson, J.B. Kopp, Am. J. Physiol. Cell Physiol. 299 (2010) C464.
[2] S. Dharia, H.E. Ayliffe, R.D. Rabbitt, Lab Chip 9 (2009) 3370.
[3] P. Seriburi, S. McGuire, A. Shastry, K.F. Bohringer, D.R. Meldruim, Anal. Chem. 80 (2008) 3677.
[4] N. Kataoka, K. Iwaki, K. Hashimoto, S. Mochizuki, Y. Ogasawara, M. Sato, K. Tsujioka, F. Kajiya, Proc. Natl. Acad. Sci. U.S.A. 99 (2002) 15638.
[5] P. Wolf, A. Rothermel, A.G. Beck-Sickinger, A.A. Robitzki, Biosens. Bioelectron. 24 (2008) 253.
[6] C.R. Keese, J. Wegener, S.R. Walker, L. Giaever, Proc. Natl. Acad. Sci. U.S.A. 101 (2004) 1554.
[7] P.A. Vogel, S.T. Halpin, R.S. Martin, D.M. Spence, Anal. Chem. 83 (2011) 4296.
[8] L. Ceriotti, J. Ponti, P. Colpo, E. Sabbioni, F. Rossi, Biosens. Bioelectron. 22 (2007) 3057.
[9] R.M. Wightman, Science 311 (2006) 1570.
[10] C. Amatore, S. Arbault, M. Guille, F. Lemaitre, Chem. Rev. 108 (2008) 2585.
[11] X.J. Chen, A.C. West, D.M. Cropek, S. Banta, Anal. Chem. 80 (2008) 9622.
[12] P. Manning, C.J. McNeil, J.M. Cooper, E.W. Hillhouse, Free Radic. Biol. Med. 24 (1998) 1304.
[13] S. Shleev, J. Wettero, K.E. Magnusson, T. Ruzgas, Biosens. Bioelectron. 22 (2006) 213.
[14] B. Ge, F. Lisdat, Anal. Chim. Acta 454 (2002) 53.
[15] R. Buettemeyer, A.W. Philipp, L. Schlenzka, J.W. Mall, M. Beissenhirtz, F. Lisdat, Transplant. Proc. 35 (2003) 3116.
[16] S.C. Chang, N. Pereira-Rodrigues, J.R. Henderson, A. Cole, F. Bedioui, C.J. McNeil, Biosens. Bioelectron. 21 (2005) 917.
[17] S. Gaspar, C. Niculite, D. Cucu, I. Marcu, Biosens. Bioelectron. 25 (2010) 1729.
[18] S. Shleev, J. Wettero, K.E. Magnusson, T. Ruzgas, Cell Biol. Int. 32 (2008) 1486.
[19] M. Brischwein, E.R. Motrescu, E. Cabala, A.M. Otto, H. Grothe, B. Wolf, Lab Chip 3 (2003) 234.
[20] M. van Leeuwen, E.E. Krommenhoek, J.J. Heijnen, H. Gardeniers, L.A. van der Wielen, W.M. van Gulik, Biotechnol. Progr. 26 (2010) 293.
[21] J. Gottschamel, L. Richter, A. Mak, C. Jungreuthmayer, G. Birnbaumer, M. Milnera, H. Bruckl, P. Ertl, Anal. Chem. 81 (2009) 8503.
[22] D. Hernandez-Garcia, C.D. Wood, S. Castro-Obregon, L. Covarrubias, Free Radic. Biol. Med. 49 (2010) 130.
[23] M. Davalos, S. Konno, M. Eshghi, M. Choudhury, J. Endourol. 24 (2010) 339.
[24] B.K. Canales, L. Anderson, L. Higgins, K. Ensrud-Bowlin, K.P. Roberts, B.L. Wu, I.W. Kim, M. Monga, Urology 76 (2010).
[25] J.M. Ouyang, R. Yang, J. Tan, Prog. Chem. 22 (2010) 1665.
[26] C. Guo, K.E. McMartin, Toxicology 208 (2005) 347.
[27] P.L. McNeil, E. Warder, J. Cell Biol. 88 (1987) 669.
[28] A.R. Jayakumar, K.V.R. Rao, K.S. Panickar, M. Moriyama, P.V.B. Reddy, M.D. Norenberg, J. Neuropathol. Exp. Neurol. 67 (2008) 417.
[29] C. Miller, L. Kennington, R. Cooney, Y. Kohjimoto, L.C. Cao, T. Honeyman, J. Pullman, J. Jonassen, C. Scheid, Toxicol. Appl. Pharmacol. 162 (2000) 132.
[30] M. Moriyama, A.R. Jayakumar, X.Y. Tong, M.D. Norenberg, J. Neurosci. Res. 88 (2010) 2450.